



Synthesis of Fe₃O₄/Au/Eu(TTA)₃-folate nanomaterial for applications in biomedical

Hoang Thi Khuyen^{1,2*}, Tran Thu Huong^{1,2}, Pham Thi Lien^{1,2}, Nguyen Thanh Huong^{1,2}, Nguyen Vu^{1,2}

¹ Institute of Materials Science, Vietnam Academy of Science and Technology, 18 Hoang Quoc Viet, Cau Giay, Hanoi, Vietnam

² Graduate University of Science and Technology, Vietnam Academy of Science and Technology, 18 Hoang Quoc Viet, Cau Giay, Hanoi, Vietnam

*Email: khuyenht@ims.vast.ac.vn; khuyenhtims@gmail.com

ARTICLE INFO

Received: 12/3/2021

Accepted: 15/6/2021

Published: 15/10/2021

Keywords:

Functionalization, multifunctional, nanocomposite, Eu(TTA)₃, folate,

ABSTRACT

The Fe₃O₄/Au/Eu(TTA)₃ nanocomposite was functionalized with amino groups, which folic acid was attached to the amino groups to permit targeting of certain cancer cell lines that express high levels of folate receptor. In this paper, a Fe₃O₄/Au/Eu(TTA)₃-folate nanocomplex was successfully synthesized. The as-synthesized material has small size from 75 to 100 nm in diameter and good dispersity in solution. In addition, this nanocomplex exhibits strong emission at $\lambda_{max} = 614$ nm, superparamagnetic properties and high biocompatibility.

Introduction

In recent years, nanotechnology has developed rapidly, allowing the design and synthesis of a number of nanostructures (from a few to several hundred nanometer) for biomedical applications. Multifunctional nanomaterials are one of promising groups for combined diagnostics and therapeutics [1-3].

A huge number of scientific articles have been published dealing with the multifunctional nanomaterials, such as luminescent-magnetic plasmonic-magnetic and luminescent-plasmonic nanomaterials and their prospects for applications in biomedicine [4-9]. Among the luminescent materials for photonics and biomedicine, luminescent rare-earth complexes of europium(III) have attracted great attention, due to their excellent optical properties. Their advantages include large Stokes shift, narrow emission spectrum and long fluorescence lifetime [10-14]. In order to obtain the desired biomedical

multifunctional nanoproducts, besides a good control of the composite, size and shape of nanoparticles, a surface treatment technology for functionalization and biocompatibility is still a challenge. Different functionalized groups, such as amine, carboxyl, hydroxyl groups... can be attached to the surface of nanostructures through co-condensation and surface modification. The surface functionalization has enabled the effective applications of nanomaterials in biomedical fields, such as targeted drug delivery, luminescent label, bioimaging, diagnostic and treatment [15, 16].

Recently, the study of targeting the folate receptor using folic acid has been considered as a promising strategy for the treatment of inflammation or cancer with a variety of drugs in clinical trials. Some reports show that folic acid containing an α -carboxylic acid group allows for simple conjugation and chemical reactions, contributing to good efficacy in drug delivery and disease treatment [17-20].

In this paper, we will present some results of synthesis and functionalization of folic acid of multifunctional nanomaterials that consist of luminescent europium(III) complex with organic 3-thenoyltrifluoroacetone ($\text{Eu}(\text{TTA})_3$) ligand combined with magnetic Fe_3O_4 and plasmonic Au nanoparticles (FGET-folate) to achieve specific targeting on cells. Some characteristics and properties of this nanocomposite were discussed to guide applications in biomedicine.

Experimental

Experiments on synthesis, functionalization and conjugation of the FGET-folate nanomaterial were performed with the following chemicals: $\text{EuCl}_3 \cdot 6\text{H}_2\text{O}$, tri-*n*-octylphosphineoxide (TOPO), 3-thenoyltrifluoroacetone (TTA), $\text{HAuCl}_4 \cdot 3\text{H}_2\text{O}$, (3-mercaptopropyl) trimethoxysilane (MCPMS), ammonium hydroxide (NH_4OH), sodium hydroxide (NaOH), $\text{FeCl}_3 \cdot 6\text{H}_2\text{O}$, tetraethyl orthosilicate (TEOS), 3-(triethoxysilyl)-propylamine (TESPA), *N,N*-dicyclohexylcarbodiimide (DCC), folic acid (FA), dimethyl sulfoxide (DMSO), ascorbic acid (AA), hexadecyltrimethylammonium bromide (CTAB) from Aldrich-Sigma. *N*-hydroxysuccinimide (NHS), $\text{FeCl}_2 \cdot 4\text{H}_2\text{O}$ from Acros. Tri-sodium citrate dihydrate (TCS), ethanol from Merck. All chemicals are of analytical grade. Deionized water (DI) was used in the synthesis of the nanoparticles.

Multifunctional $\text{Fe}_3\text{O}_4/\text{Au}/\text{Eu}(\text{TTA})_3$ nanomaterial (FGET) was synthesized by Stober method in solution according to the reference procedure [12]. A brief summary of the process is as follows: Fe_3O_4 nanoparticles were synthesized by coprecipitation method from a mixture of $\text{FeCl}_3 \cdot 6\text{H}_2\text{O}$, $\text{FeCl}_2 \cdot 4\text{H}_2\text{O}$ and NaOH . 500 μl of MCPMS/TEOS at a ratio of 1/1 in molarity was added to the solution of TCS stabilized Fe_3O_4 nanoparticles at a concentration of 5mg/ml. The solution was stirred well and adjusted to $\text{pH}=8.5$. Then, 0.01M CTAB, 0.01M HAuCl_4 and 0.1M AA solutions were added, respectively. 50 μl TESPAs and $\text{Eu}(\text{TTA})_3$ complex that were prepared by a mixture of $\text{EuCl}_3 \cdot 6\text{H}_2\text{O}$, TOPO và TTA in the ratio 1:3:3 in terms of moles were added and stirred for 6 hours. After a cleaning process, the FGET nanocomposite was dispersed in ethanol and functionalized with folic acid according to the following steps: 100mg FA was dissolved in 10ml DMSO solvent. An amount of NHS and DCC was added to the solution in a molar ratio of FA/NHS/DCC of 1/3/1. The reaction was carried out in dark at room temperature for 6 hours. Next, the FGET nanocomposite was added and

stirring was maintained for 12 hours. The synthesized FGET-Folate nanocomplex was cleaned by magnetic separation by a magnet and dried at 60°C for 24 hours.

The morphology of the nanomaterial was observed on a field emission electron microscope (FESEM, Hitachi-S4800). The crystal structure was analyzed by X-ray diffraction pattern on a Bruker D8 Advance XRD instrument. FTIR spectra were measured by a Nexus 670 ThermoNicolet Fourier Transform Infrared Spectrometer. The UV-VIS absorption spectrum of the studied sample was measured by the UV-VIS Biochrom s60 instrument system. The fluorescence spectra were measured by the IHR 550 Hobira Jobin Yvon (USA). Magnetic measurement was studied by a Vibration Sample Magnetometer (VMS). Fluorescence image was observed by a Nikon DS-Qi2 fluorescence microscope.

Results and discussion

The chemical structure of the $\text{Eu}(\text{III})$ complex with organic ligands of 3-thenoyltrifluoroacetone ($\text{Eu}(\text{TTA})_3$) was illustrated in figure 1(a). This luminescent complex was incorporated in the FGET nanocomposite whose structure is illustrated in figure 1(b).

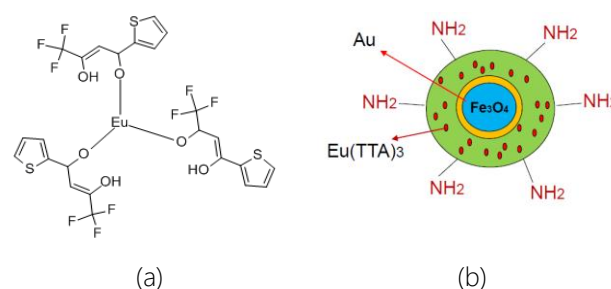


Figure 1: (a)- Chemical structure of the luminescent $\text{Eu}(\text{TTA})_3$ complex and (b)- of FGET nanocomposite

The functionalization reaction of FGET nanocomposite with FA according to the reaction scheme is presented in figure 2.

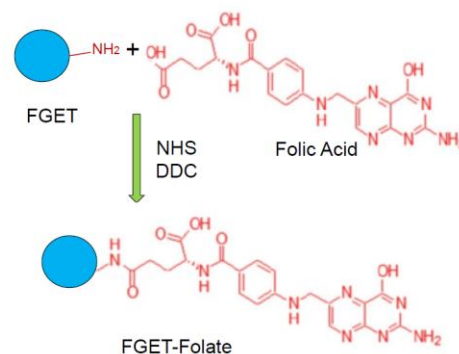


Figure 2: Schematic of the functionalization synthesis of

FGET-Folate nanocomplex

Figure 3 presents some sample images of the as-synthesized FGET-Folate nanocomplex. From experiment, the obtained sample is black, has a good dispersion in liquid medium such as water and ethanol. It has a rather slow sedimentation rate (figure 3(a)). Nanoparticles tend to be attracted closer to the direction of the magnet (figure 3(b)). This proves that the synthesized FGET-Folate nanocomplex has magnetic properties, due to the presence of the iron oxide nanoparticles.

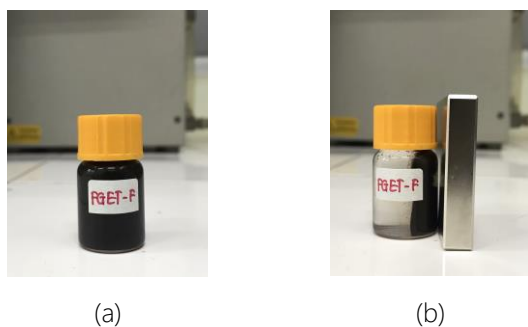


Figure 3: Sample image of FGET nanocomposite

The morphology and size of the FGET nanocomposites were observed by FESEM image (figure 4). The result shows that the material has a spherical structure, the particles size is distributed in the range of 75nm-100nm. For biomedical applications such as intra- or extracellular fluorescence label, drug delivery or therapeutics, this size is perfectly suitable.

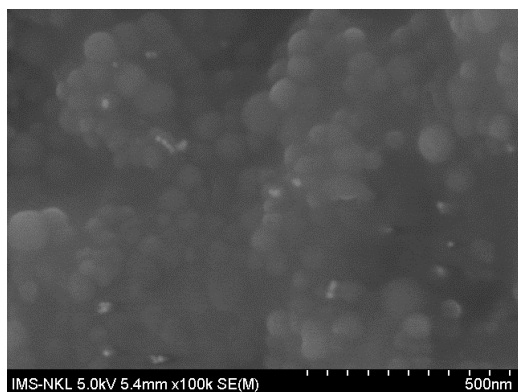


Figure 4: FESEM image of FGET nanocomposites

Figure 5 shows UV-VIS absorption spectrum of the FGET-Folate nanocomplex. From the result, two spectral bands are formed. The first band in the ultraviolet region with a maximum absorption at 383nm is exhibited by the absorption of the luminescent $\text{Eu}(\text{TTA})_3$ complex. The second band appears in the visible region with a maximum absorption wavelength at 530nm. This is the plasmon absorption band of the gold nanoparticles. This broad

spectrum from the ultraviolet to the visible region may allow to overcome the ultraviolet excitation limitations of rare-earth fluorescent materials.

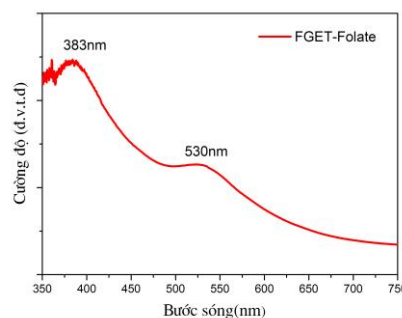


Figure 5: UV-VIS absorption spectra of FGET-Folate nanocomplex

The X-ray diffraction pattern of the FGET-Folate nanocomplex is shown in the figure 6. The X-ray diffraction peaks are observed at $2\theta=30.3^\circ$, 35.7° , 43.5° , 57.5° and 62.8° , respectively, corresponding to the lattice surface of (220), (311), (400), (511) and (440). These diffraction characterize the face-centered cubic structure of Fe_3O_4 (according to the International Center for Diffraction Data card 19-629). The rather sharp diffraction peaks indicate that the nanoparticles are well crystallized. Besides, a wide band corresponding to 2θ from 20° to 30° is also observed due to an amorphous structure of the functionalized organic layer with folic acid.

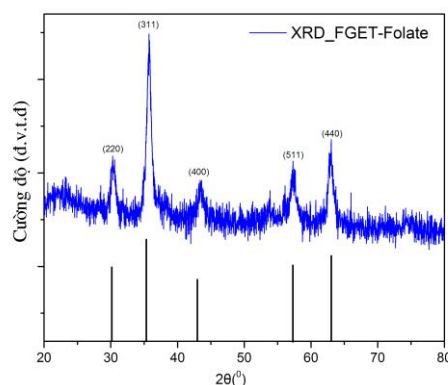


Figure 6: X-ray diffraction pattern of FGET-Folate nanocomplex

Figure 7 shows the FTIR spectra of folic acid (line a), FGET nanocomposite (line b) and FGET-Folate nanocomplex (line c). The FTIR spectra of folic acid (line a) shows strong characteristic peaks at 3435 cm^{-1} corresponding to the oscillations of the O-H group of carboxylic acid and N-H group (amine group). The

peaks at 1651 cm^{-1} and 1435 cm^{-1} , respectively, are related to the N-H (bending) oscillation of the CONH bond and the C=O bond of the α -carboxyl group. The lines (b) and (c) show strong band in the low wave number region ($500\text{-}1000\text{ cm}^{-1}$) associated with Eu-O bond. Besides, the Fe-O bond also corresponds to low frequency oscillations around 570 cm^{-1} . The results of the spectrum analysis show that the peaks at wave numbers of 3435 cm^{-1} , 1634 cm^{-1} and 1437 cm^{-1} , respectively, correspond to the oscillations of the NH bond (amine group), C=O (ketone group) and CF (TTA organic ligand). The oscillation peaks at the 1040 cm^{-1} (line b) and 1013 cm^{-1} (line c) are related to Si-O-Si bond, respectively. The band appearing from 1900 cm^{-1} to 2300 cm^{-1} in the both samples is related to the oscillations of the Si-H bond [21]. This demonstrated the formation of a functionalized layer of silica in the nanocomplex. Compared with the FGET nanocomposite, a peak at 1507 cm^{-1} indicates that the amide bond was formed after the functionalization with folic acid.

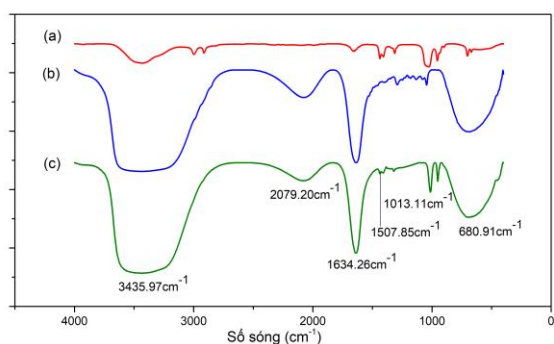


Figure 7: FTIR spectra of (a)- folic acid, (b)- FGET nanocomposite and (c)- FGET-Folate nanocomplex

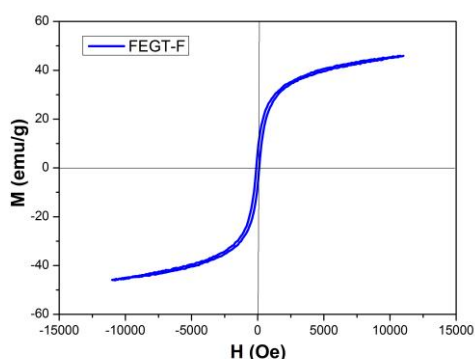


Figure 8: Hysteresis curve of FGET-Folate nanocomplex

The hysteresis curve of the synthesized FGET-Folate nanocomplex is shown in figure 8. This measurement was performed at room temperature, with an applied

magnetic field between $+10000\text{ Oe}$ and -10000 Oe .

The result shows that the FGET-Folate nanocomplex exhibits superparamagnetic properties. At the applied magnetic field of 10000 Oe , the magnetization of the sample is about $45,94\text{ (emu/g)}$. In particular, the coercive force value is low (H_c is about a few Oe). The superparamagnetic property has important implications for biomedical applications. The nanomaterials are easily dispersed in solution or controlled the targeted drug delivery and hyperthermia using an external magnetic field.

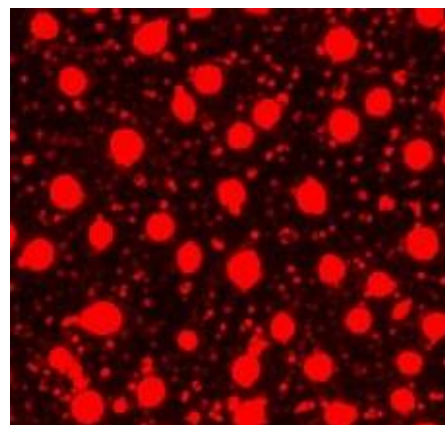


Figure 9: Fluorescence microscopy image of FGET-Folate nanocomplex

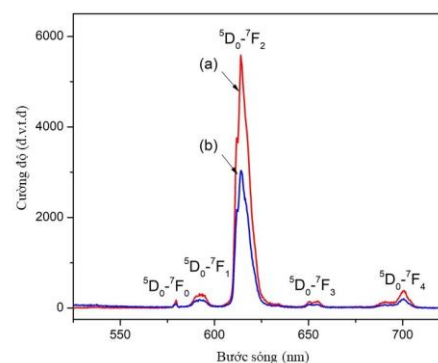


Figure 10: Luminescence spectra of (a)- FGET nanocomposite and (b)- FGET-Folate nanocomplex, under an excitation at 355 nm

Figure 9 presents the fluorescence microscopy image of the FGET-Folate nanocomplex material. As observed by fluorescence microscopy, the nanomaterial is capable of strong emitting red luminescence. This result is also clearly demonstrated by the luminescent spectra of the studied samples. Figure 10(a) and 10(b) show the luminescence spectra under an excitation at 355 nm of the FGET nanocomposite and FGET-Folate nanocomplex, respectively. Compared with the luminescence spectra of the FGET nanocomposite sample, the functionalization with folic acid has not

much influence on the spectra form. After functionalization with folic acid, the nanomaterial has good luminescence with narrow emission characteristic with transitions of $^5D_0 \rightarrow ^7F_j$ ($j = 1, 2, 3$ and 4) of Eu(III) ion. The maximum emission at $\lambda_{\text{emi}}=614\text{nm}$. However, a decrease in intensity was observed due to a dilution effect.

Conclusion

The novel FGET-Folate nanocomplex has been successfully synthesized. The nanomaterial has a small particle size in the range of 75-100nm. It is well dispersed in liquid media such as water or ethanol. The absorption spectra is extended towards visible region. After functionalization with folic acid, the FGET-Folate nanocomplex has good red luminescence, superparamagnetic properties and simultaneously contains functional groups such as $-\text{NH}_2$ and $-\text{COOH}$ which favors a conjugation with biomolecules. This results have created a promising nanocomposite for imaging diagnostics, which can combine phototherapy, thermotherapy and specific targeted drug delivery on folate receptor-expressing cells.

Acknowledgments

This research is funded by Vietnam National Foundation for Science and Technology Development (NAFOSTED) under grant number 103.03-2017.52

References

1. Madaswamy S Muthu, Lin Mei, Si Shen Feng, *Nanomedicine* 9 (9) (2014) 1277-1280. <https://doi.org/10.2217/nnm.14.83>
2. Maria Mir, Saba Ishtiaq, Samreen Rabia, Maryam Khatoon, Ahmad Zeb, Gul Majid Khan, Asim ur Rehman and Fakhar ud Din, *Nanoscale Research Letters*, 12 (1) (2017) 500. <https://10.1186/s11671-017-2249-8>.
3. M. Angelakeris, *Biochimica et Biophysica Acta (BBA) - General Subjects* 1861 (2017) 1642-1651. <https://10.1016/j.bbagen.2017.02.022>.
4. X. Yao, X. Niu, K. Ma, P. Huang, J. Grothe, S. Kaskel and Y. Zhu, *Advanced Science News* 13 (2017) 1602225. <https://doi.org/10.1002/sml.201602225>.
5. H. T. Khuyen, N. T. Lan, N. Vu, P. T. Lien, T. T. Hường, N. T. Huong, D. T. A. Thu, T. T. K. Chi, N. T. H. Le, V. Th. Ha, P. D. Roan, *Vietnam Journal of Chemistry*, 55(3e12) (2017) 154-157.
6. P. T. Lien, N. T. Huong, T. T. Huong, H. T. Khuyen, N. T. N. Anh, N. D. Van, N. N. Tuan, V. X. Nghia, and L. Q. Minh, *Journal of Nanomaterials*, Volume 2019 (2019) 3858439. <https://doi.org/10.1155/2019/3858439>
7. Ana Espinosa, Riccardo Di Corato, Jelena Kolosnjaj-Tabi, Patrice Flaud, Teresa Pellegrino and Claire Wilhelm, *ACS Nano* 10 (2016) 2436–2446. <https://10.1021/acsnano.5b07249>.
8. H. T. Khuyen, T. T. Huong, D. K. Tung, P. T. Thu, N. T. Binh, L. Q. Minh, T. K. Anh, L. N. Diep, N. T. H. Lien and P. A. Tuan, *Journal of Electronic Materials* 45 (2016) 4400-4406. <https://10.1007/s11664-016-4583-5>
9. L. M. Quynh, C. T. Dung, B. T. Mai, H. V. Huy, N. Q. Loc, N. Q. Hoa, P. T. Thach, B. V. Anh, C. T. Thao, N. H. Nam, H. T. M. Nhung, N. N. Long & L. V. Vu, *Journal of immunoassay and immunochemistry*, 39 (3) (2018) 308–322.
10. Q. Minh L., T. Huong T., T. Huong N., T. Khuyen H., T. Binh N., K. Tung D., K. Anh T., D. Hien N., T. Luan L., T. Quy N., M. Dung D., N. A. Thu N., and V. Man N., *Adv. Nat. Sci.: Nanosci. Nanotechnol.*, 3 (2012) 035003. <https://10.1007/s11664-016-4583-5>.
11. Syamchand, S.S. and G. Sony, *Journal of Luminescence* 165 (2015) 190-215. <https://10.1016/J.JLUMIN.2015.04.042>.
12. H. T. Khuyen, T. T. Huong, N. T. Huong, V. T. T. Ha, N. D. Van, V. X. Nghia, T. K. Anh, L. Q. Minh, *Optical Materials* Volume 109 (2020) 110229. <https://doi.org/10.1016/j.optmat.2020.110229>.
13. Comby, S., et al., *Inorganic Chemistry* 53(4) (2014) 1867-1879. <https://doi.org/10.1021/ic4023568>
14. Jean-Claude G. Bünzli, *Journal of Luminescence* 170 (2016) 866–878. <https://10.1016/j.jlum.2015.07.033>.
15. Vasudevanpillai Biju, *Chem. Soc. Rev.* 43 (2014) 744. <https://10.1039/c3cs60273g>.
16. Wang, L., et al., *Nano Research* 1(2) (2008) 99-115.
17. T. T. N. Huyen, B. T. T. Ha, D. D. Quang, L. T. T. Huong, P. T. T. Huong, *Vietnam Journal of Science and Technology* 62(12) (2020) 7-11.
18. H. T. Phuong, T. T. Huong, H. T. Khuyen, L. T. Vinh, D. T. Thao, N. T. Huong, P. T. Lien and L. Q. Minh, *Journal of Rare earth* 37(11) (2019) 1183-1187. <https://doi.org/10.1016/j.jre.2019.01.005>.
19. L. T. T. Huong, N. H. Nam, D. H. Doan, H. T. M. Nhung, B. T. Quang, P. H. Nam, P. Q. Thong, N. X. Phuc, H. P.

20. Thu, *Materials Chemistry and Physics* 172 (2016) 98-104.
<https://doi.org/10.1016/j.matchemphys.2015.12.065>.
21. Rachel L. Merzel, Carolina Frey, Junjie Chen, Rachel Garn, Mallory van Dongen, Casey A. Dougherty, Ananda Kumar Kandaluru, Philip S. Low, E. Neil G. Marsh and Mark M. Banaszak Holl, *Bioconjugate Chem.* 28 9 (2017) 2350–2360.
<https://doi.org/10.1021/acs.bioconjchem.7b00373>.
22. Kirill O. Bugaev, Anastasia A. Zelenina, and Vladimir A. Volodin, *International Journal of Spectroscopy*, Volume 2012 (2012).
<https://doi.org/10.1155/2012/281851>.